Wong *et al. Soft Sci* 2021;1:Accept
DOI: 10.20517/ss.2021.09

Soft Science

Research Article

Tattoo-like Epidermal Electronics as Skin Sensors for Human Machine Interfaces

Tsz Hung Wong[1,#], Chun Ki Yiu[1,5,#], Jingkun Zhou[1,5,#], Zhen Song[2,3,#], Yiming Liu[1], Ling Zhao[1], Kuanming Yao[1], Wooyoung Park[1], Woojung Yoo[1], Enming Song[4]*, Zhaoqian Xie[2,3]*, Xinge Yu[1]*

[1]Department of Biomedical Engineering, City University of Hong Kong, Hong Kong 999077, China.
[2]State Key Laboratory of Structural Analysis for Industrial Equipment, Department of Engineering Mechanics, Dalian University of Technology, Dalian 116024, China.
[3]Ningbo Institute of Dalian University of Technology, Ningbo 315016, China.
[4]Institute of Optoelectronics, Fudan University, Shanghai 200438, China.
[5]Hong Kong Centre for Cerebro-Cardiovascular Health Engineering, Hong Kong 999077, China.
#These authors contributed equally: Tsz Hung Wong, Chun Ki Yiu, Jingkun Zhou, and Zhen Song

***Corresponding to:** Prof. Enming Song, Shanghai Frontiers Science Research Base of Intelligent Optoelectronics and Perception, Institute of Optoelectronics, Fudan University, Shanghai 200433, China. E-mail: sem@fudan.edu.cn; Prof. Zhaoqian Xie, State Key Laboratory of Structural Analysis for Industrial Equipment, Department of Engineering Mechanics, Dalian University of Technology, Dalian 116024, China. E-mail: zxie@dlut.edu.cn; Prof. Xinge Yu, Department of Biomedical Engineering, City University of Hong Kong, Hong Kong 999077, China. E-mail: xingeyu@cityu.edu.hk

How to cite this article: Wong T, Yiu C, Zhou J, Song Z, Liu Y, Zhao L, Yao K, Park W, Yoo W, Song E, Xie Z, Yu X. Tattoo-like Epidermal Electronics as Skin Sensors for Human Machine Interfaces. *Soft Sci* 2021;1:[Accept]. https://dx.doi.org/10.20517/ss.2021.09

Received: 30 Jul 2021 **Revised:** 22 Sep 2021 **Accepted:** 23 Sep 2021 **First online:** 23 Sep 2021

Abstract

Flexible electronic skin (e-skin) has been proved for their diverse applications in prosthesis sensing, body-motion monitoring, and the human-machine interfaces, due to their superior mechanical properties and commendable electrical characteristics. However, the reported e-skins are still relatively thick(>10μm) and uncomfortable for long-term use on the human body. Herein, an ultra-thin, skin-integrated designs of strain sensor with miniaturized dimensions, based on the piezoresistive effect, with excellent stability and robustness are introduced. Fractal curve-shaped Au electrode in a serpentine format, which is the dominant component of the strain sensor, is sensitive to the ambient strain variation and able to turn the mechanical motion into stable electrical signal output. With the advanced design of the metallic electrodes, the device presents good operational stability and excellent mechanical tolerance towards bending, stretching, and twisting. The stain sensor allows intimate mounting onto the human epidermal surface for detecting body motions. By adopting the liquid bandage (LB) as the encapsulation layers, the device owns an ultrathin thickness (6.2 μm), high sensitivity towards mechanical deformations, which is able to clearly detect motions such as walking, finger bending, and human pulse rate with identifiable electrical signals. Furthermore, the tattoo-like strain sensor is applied in robotic control by tracing finger bending motion and result in smooth control of a robotic hand nearly without any detention. The e-skin has exhibited a great potential in wearable electronics and the human-machine interfaces.

Keywords: Skin-integrated electronics, ultrathin, excellent repeatability, fractal design, stretchable electronics.

INTRODUCTION

Recently, epidermal electronics have attracted much attention around the world for its excellent mechanical properties and electronic characteristics[1-10]. Up to now, extensive flexible strain sensors have been developed based on various operational principles, such as piezoelectricity[11-14], triboelectricity[15-17], piezoresistance[18-21][22], e.g. Among the reported strain sensors, piezoelectric and triboelectric devices have raised extremely high interests for their natural characteristics in self powering[23-31]. However, the instantaneous electrical signals and fast attenuation of electrical performance significantly limits their further development in the application of e-skin[32]. Distinguished with the self-powered strain sensors, e-skin, based on piezoresistive effect, provides functions closer to human skin, capable of real-time detecting strain variations accurately[33-38]. Resistance change of the piezoresistive in e-skin can be conveniently transformed into voltage changes via real-time electrical monitoring of the sensor, then recognized by microcontroller for later robotic control.

Benefited from the fast development of materials science, many piezoresistive effect-based e-skins have been reported by incorporating advanced conductive materials, such as graphene and PDMS composite[39-42], ionic conductive hydrogels[43-45], graphene coated fabric[46-48], e.g. To achieve sufficient repeatability and stability, the fabrication process of the newly-developed materials tends to require expensive equipment and rigorous experimental environment, difficult with standard facilities in academic cleanrooms. Compared to these strain sensors, e-skins based on metal electrodes can realize a low-cost fabrication but high stability and repeatability with sufficient electrical sensitivity[48]. As the noble metal, gold (Au) exhibits high oxidation resistance, suitable for fabricating the strain sensor.[49, 50] To realize the long-term utilization on the human skin surface, e-skin should fulfill several characteristics, including 1) extremely light-weight and imperceptible architectures without any limitation and influence on body motion. 2) skin-compatible interfaces to the targeted skin with a soft, curved dynamic surface in a stable, safe fashion, not easy

to split away off skin surface. 3) outstanding operational performance characteristics with high sensitivity and accuracy.

Herein, we report an ultrathin skin-integrated strain sensor based on the piezoresistive effect with excellent stability and repeatability. The key component is the Au electrode in the format of fractal curve, sensitive to the ambient strain variations. To minimize the effect of the device on the skin strain field distribution, the overall size of the sensor is designed as 5 mm × 2 mm × 6.2 μm (length × width × thickness) with a light weight of 0.204 mg. Compared with the conventional strain sensor based on piezoresistive effect, our strain sensor demonstrates superiorly tiny size and thin thickness with competitive stretching range and sensitivity (**Table S2**).[51-56] Guided by theoretical modeling, the advanced structure design enables conformal integration with the skin under large mechanical deformations. In order to yield the intimate contact on complex textures of epidermal surfaces, liquid bandage is sprayed as a connection layer between the sensors and the epidermal surface. Compared to the commonly adopted PDMS layer, the liquid bandage owns the advantages of thin thickness (1 μm), and light weight. The tight bondage between the sensors and the epidermal surface allows the users' unhindered movements and providing precise measurement of the body motions sensing in an highly accurate approach. By accurately capturing finger motions and pulse rate, the sensor provides a promising alternative for real-time monitoring human health. In addition, with signals obtained from the strain sensors, a six-degree-of-freedom prosthetic arm is then used to imitate the motion of the human hand, by applying to program for sensitivity and detection adjustment.

DISCUSSION AND RESULT

Fig. 1a presents the schematic diagram of the strain sensor. To ensure the surface smoothness and the fabrication compatibility, a quartz glass was used as the substrate first, with a spin coated Poly(methyl methacrylate) (PMMA) thin film on top as sacrificial layer and a thin polyimide (PI) film as metal electrode supporting layer. Metallic layers (Cr/Au) were deposited on the PI and patterned by photolithography, serving as the functional electrode for strain change detection. Spin-casting another PI

and selectively dry etching by Reactive Ion Etching (RIE) provided a top encapsulation layer for building a robust system. Dissolving the PMMA with acetone enabled transfer printing of the electrode onto the targeted skin area with pre-sprayed liquid bandage through a water-soluble tape (WST). Finally, an additional layer of liquid bandage was sprayed on top of the electronics to encapsulate the exposed gold electrode. The device features by the filamentary fractal design of the gold electrode (200 nm) and an ultrathin and stretchable encapsulation layer (liquid bandage, 1 μm) to enhance the overall flexibility and biaxial stretchability of the system (**Fig. 1b**). The liquid bandage acts as a tight adhesion and robust encapsulation of the strain sensor. A sensor is mounted on a volunteer's forearm over 12 hours, during the period, the volunteer is allowed to perform any daily movements, like walking, running, and twisting his forearm. After 12 hours, the sensor is still mounted on his forearm and there is not any sign of flaking. According to the experimental studies, the ultrathin encapsulation layers can provide an excellent protection of the gold electrode underneath, and the sensor could endure various mechanical forces, like continuous rubbing, while remaining undamaged (**Movie S1**). Apart from the external loads, the liquid bandage is waterproof, which could protect the sensor in the moisture environment. There is experimental study proves that, with the encapsulation of the liquid bandage, the sensor is approximately unaffected in a watery environment, where the change in the electrical signal ($\Delta R/R_0$) is less than ± 0.02% (**Fig. S1**). This tight adhesion and waterproof capability of the liquid bandage allow the strain sensor working unaffectedly under large body movements and sweated skin surface. The overall dimension of the strain sensor is 5 mm × 2 mm (length × width) and a 6.2 μm of thickness, making it more convenient and comfortable as attached to the human body, as shown in **Fig. 1c**. Compared with the recent reported piezoresistive strain sensors, our device demonstrates superiorly tiny size with competitive stretching range and sensitivity, shown in **Table S1**. The ultra-thin design combing with filamentary fractal Au wires allows the device to be stretched, bent and twisted for seamless and conformal integration onto curvilinear surfaces of human epidermis (**Fig. 1d** and **1e**). It is tested that most of the skin surface would stretch within 20%, without any external stretching (Table S2). It indicates that the strain sensor could be mounted on most of the body parts for the body movement monitoring. The finite element analysis (FEA) shows that the maximum equivalent strain in Au is less than the yield strain 0.3% for the device under 280° bending (bending radius ~2.7 mm), 20%

stretching, and 90° twisting (**Fig. 1d**). These results highlight the robust, and stretchable device which can operate under realistic physiological loads.

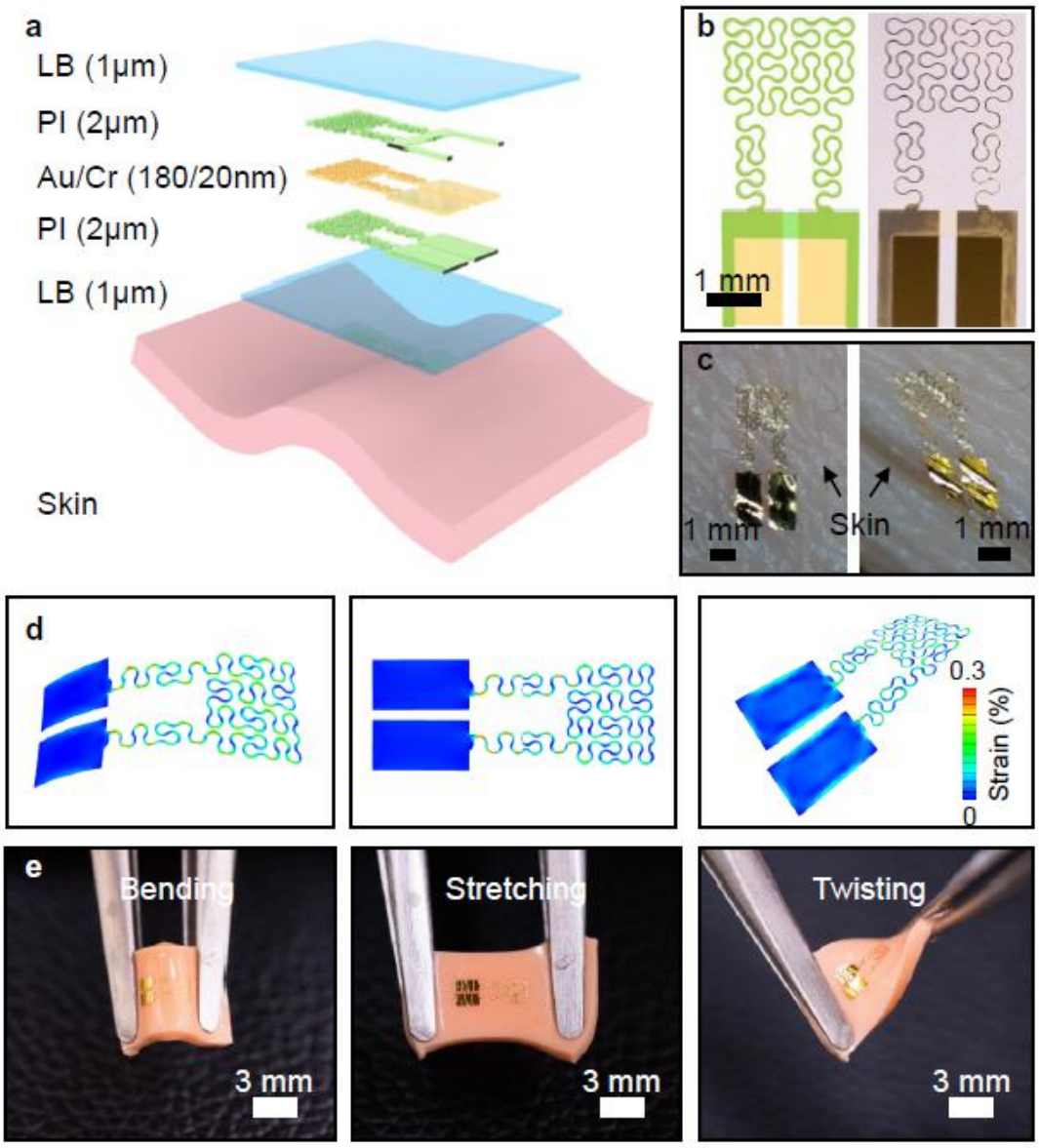

Fig. 1. Flexible, ultrathin, skin-integrated, and Au-based strain sensor. (**a**) Schematic diagram of the strain sensor. (**b**) The optical image of the patterned Au/Cr electrode design. (**c**) Optical image of the strain sensor mounted on the human epidermal surface. (**d**) FEA results of strain distribution on strain sensor under stretching, twisting, and bending. (**e**) Optical image of the strain sensor attached on a pink PDMS surface with three mechanical deformations, including bending, stretching, and twisting.

Fig. 2a and **2b** present the electrical signal ($\Delta R/R_0$) as a function of strain variation under the static state along length and width, respectively. It is obvious that the electrical response increases linearly with the increase of the strain along the two directions. At the strain change of 20%, the values of $\Delta R/R_0$ can reach to 0.76% and 0.61% under longitudinal and transverse tensions, respectively. It is proved that the strain sensor is sensitive to both longitudinal and transverse strain and it is able to function at the 20% strain at either direction. To investigate the frequency effect on the electrical signal, the device was tested under a constant strain variation (12.5%) with different frequencies from 1 Hz to 6 Hz, fully covering the frequencies triggered by human daily motions, as shown in **Fig. 2c**. It is found that the low frequency has no effect on the electrical response of the device due to its fast response time (0.04 s) (**Fig. 2d**). To demonstrate the high durability of the strain sensor, fatigue tests were conducted with repeated stretching for 150 cycles at 1 Hz under 11.8% strain (**Fig. 2e**) with electrical signals ranging from 0% to 0.4% (**Fig. 2f**). The results prove that the strain sensor is tough enough to endure highly intensive stretching and maintain stable electrical signal outputs.

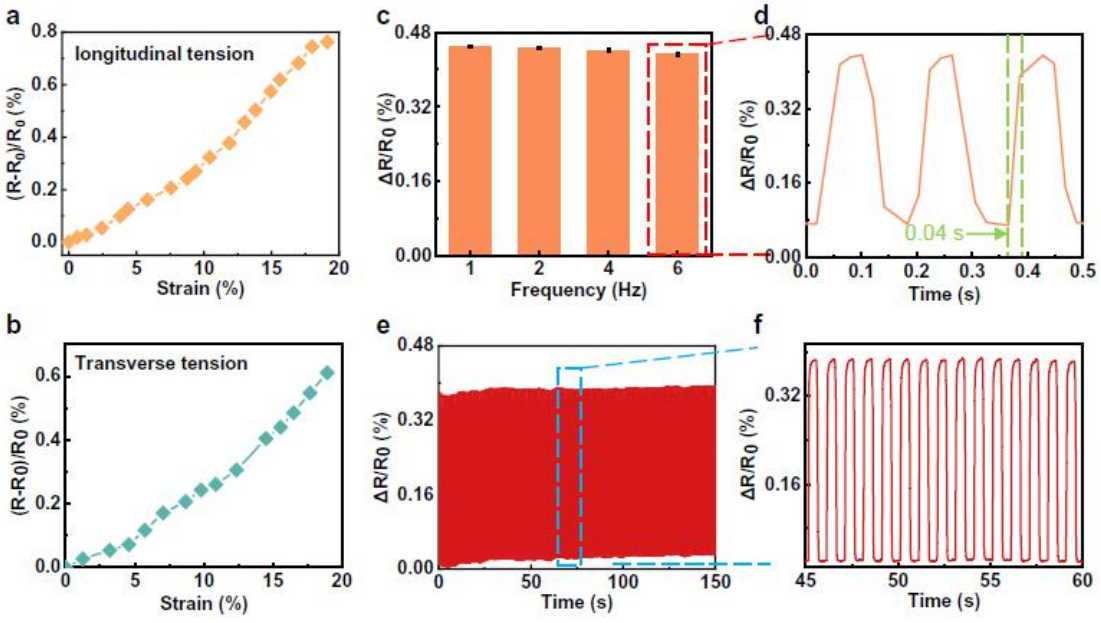

Fig. 2. The electrical characteristics of the strain sensor. (**a**) Electrical signals ($\Delta R/R_0$) of the strain sensor at different longitudinal tensions. (**b**) Electrical signals ($\Delta R/R_0$) of the strain sensor at different transverse tensions. (**c**, **d**) Electrical signals ($\Delta R/R_0$) of the strain sensor at different frequencies under 12.5%strain and its detailed signals at 6Hz. (**e**, **f**) Electrical signals ($\Delta R/R_0$) of the strain sensor in a fatigue test for 150 cycles and its detailed signals from a selected range.

To further demonstrate its meticulous structure, the sensor is mounted on the back of a hand (**Fig. 3a**). Due to its ultrathin thickness and good adhesion of the encapsulation layer, the device can be conformally mounted onto human skin without any delamination during stretching. As shown in **Fig. 3b**, the electrical signals ($\Delta R/R_0$) at the bending angles of 38 °, 61 °, and 90 ° are 0.121%, 0.285%, and 0.567% respectively. It proves that the strain sensor is capable of capturing small body movements and output obvious signals, which are later applied in robotics control. Shown in **Fig. 3c**, **d**, a sensor is attached onto an experimenter's wrist for pulse rate recording (given with its circuit diagram), where the measured relative voltage shows a regular variation ranging from 0% to 0.073%, along with the pulse rate. It is sensitive towards the human pulse, which demonstrates the potential of the flexible skin-integrated sensors in fields of clinical application. In **Fig. 3e**, it shows an optical image of the strain sensor mounted on a volunteer's ankle for his walking motion detection. The $\Delta R/R_0$ varies along with the paces, ranging from 0.0173% to 0.354% (**Fig. 3f**), which shows its capability of human motion capturing. Its sensitivity toward muscle contraction could be possibly applied in the field of motion detection in sports.

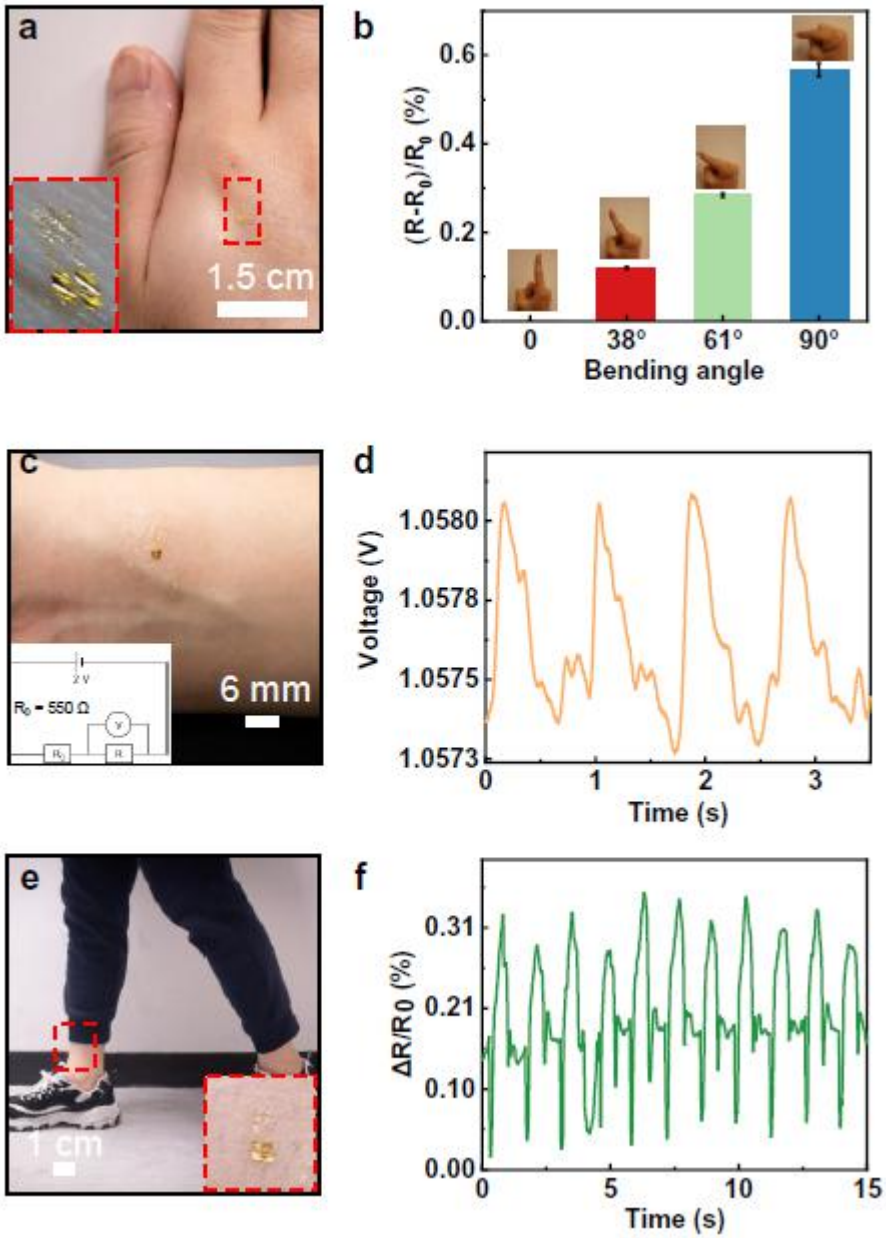

Fig. 3. The electrical signals of the flexible strain sensor under different external stimuli. (**a**) Optical image of the strain sensor mounted on the back of a hand and its enlarged optical image of the strain sensor during deformation. (**b**) Electrical signals ($\Delta R/R_0$) of the strain sensor under different finger bending angles (**c**) Optical image of strain sensor mounted on a waist for human pulse rate detection and its electrical diagram (**d**) Electrical signals (Voltage) of the strain sensor in the pulse rate test in (**c**). (**e**) Optical image of strain sensor mounted on a waist for ankle for walking motion detection. (**f**) Electrical signals ($\Delta R/R_0$) of the strain sensor under the walking motion test.

Next, the strain sensor is applied for the human-machine interface by demonstrating the robotic hand control. The schematic diagram of the testing circuit is shown in **Fig. 4a**, in which the control system is composted with six strain sensors and their corresponding amplifiers (INA828, Texas Instrument), and an Arduino board. **Fig. 4b,** and **c** show the optical images of the strain sensors mounted on the joints of a hand and circuits connected with the Arduino board (Arduino nano with ATMEGA328P-MU chip) respectively. Those sensors are mounted on the joints of the hand to capture the finger motions, which lead to a smooth control of the robotic hand. It is able to imitate the gestures of the hand almost without any detention. In **Fig. 4d**, some meaningful hand gestures, including "C", "Like you", and "Grasp", are demonstrated, which proves the high feasibility of robotic hand control. Moreover, there are three corresponding graphs underneath illustrating the electrical responses of the sensors at different hand gestures. It demonstrates the signal intensity varies with the hand's bending degree that at the fingers' complete bending and straightening conditions, the electrical signals ($\Delta R/R_0$) are 0.75% and 0.04% respectively **(Fig. 4e)**. This distinct disparity of the electrical signals leads to the accurate control of the robotic hand. To summarize, we demonstrated a human-machine interface application of the strain sensor by controlling a robotic hand in a natural and smooth approach, there is high feasibility of applying flexible strain sensors in application of human-machine interface.

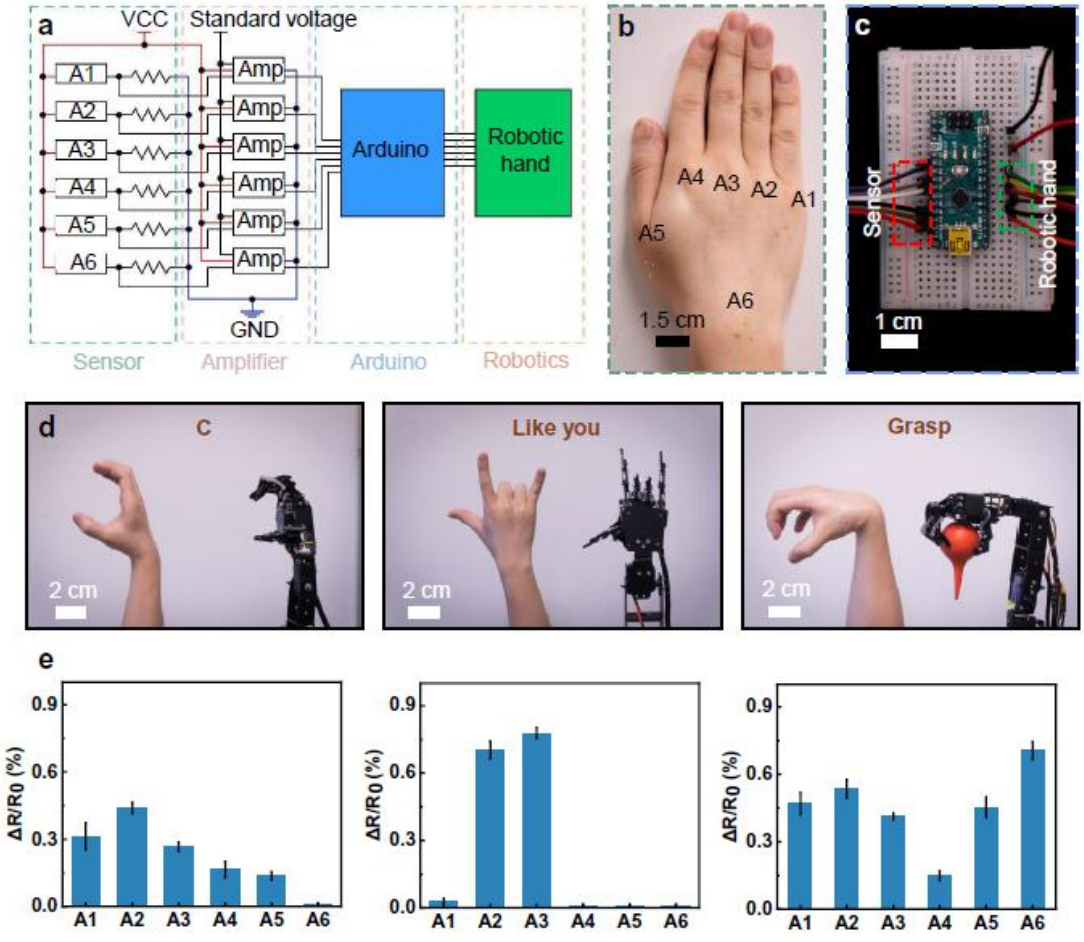

Fig. 4. Robotic hand controlling performed by the flexible strain sensors. (**a**) The schematic diagram of the testing circuit for controlling robotic hand. (**b**) Optical image of six sensors mounted on the joints of a hand for robotic hand control. (**c**) Optical image of the Arduino breadboard linked with the sensors and the robotic hand. (**d**) Optical image illustrating that the sensors control the robotic hand to make gestures of "C", "like you" and "grasp" and their corresponding electrical signals ($\Delta R/R_0$) of the sensors at different gestures (**e**).

CONCLUSION

As a summary, an ultrathin Au-based stretchable strain sensor has been developed for body motions caption and human-machine interface. It owns advantages of miniaturized dimensions (5 mm × 2 mm ×6.2 μm), skin integrability, high stability, and stretchability which allow it to be tightly mounted on the epidermal surface for body motion capturing. Its electrical signal output $\Delta R/R_0$ can raise to 0.76% and

0.61% under 20% longitudinal and transverse stretching rate, respectively, and it can undergo repeated stretching for 150 cycles at 1 Hz under 11.8 % strain. With liquid bandage as the encapsulation, the strain sensor can be tightly mounted on epidermal surface that can measure the human pulse rate and the walking motions. Furthermore, the strain sensors are applied in robotic hand control, which can imitate the finger motions of the human hand precisely, smoothly, and almost without any detention. The results in this work present the potential in body motion measuring and robotic control, which indicates a new strategy of the flexible sensors in the field of clinical application and the human-machine interface.

EXPERIMENTAL SECTION

Assembly of the tattoo-like electronic skin

First, A quartz glass was cleaned with acetone, ethanol and deionized water (DI water), sequentially. Then, PMMA solution (20mg/ml) was spin-coated onto the surface of the cleaned glass at 2000 rpm for 30s, and then baked on the hotplate at 200 °C for 20 min. The PMMA thin film served as a sacrificial layer. Afterwards, poly-amic acid solution (12.0 wt.% ± 0.5 wt.%, 3 um) was spin-coated on the PMMA sacrificial layer at 3000 rpm for 30s. Then, the PI thin film was cured on the hotplate at 250 °C for 30 min to densify. Cr (40 nm) and Au (200 nm) were next deposited on the PI film by magnetron sputtering, and then patterned with photolithography and further wet etched to form the desired pattern. The photolithography process was carried out by exposure the pre-spin-coated (3000 rpm, 30s) and soft baked (110 °C, 3 min) positive photoresist (PR, AZ 5214, AZ Electronic Materials) to the ultraviolet light for 5 s. The pattern was then developed in AZ 300MIF developer for 15s and followed with a post bake at 110 °C for 3 min. After etching the Au/Cr layer, the PR was removed with acetone, and rinsed with DI water. A second layer of PI thin film (2 μm) was then spin coated (3000 rpm, 30s) and annealed (250 °C, 30 min), followed by selectively dry etching (Oxford Plasma-Therm 790 RIE system, 200 W, 10 min). The patterned PI thin film served as the encapsulation layer covering the whole interconnects except the electrode areas. Next, the sample was immersed in acetone for 12 h to fully dissolve the PMMA layer. Water soluble tapes (WSTs) were utilized as a stamp to pick up the prepared pattern. Spray an ultrathin layer of liquid bandage (1 μm, Banitore company) on the target area of human skin. Tightly attaching the

WSTs on the target area, then dried in the air at 25 °C for 5 min formed strong mechanical bonding. Immersing the sample in water to remove the WSTs and realized stretchable electrodes on human skin. Next, a liquid bandage layer (1 μm) was sprayed on the top of the electrode. Dry the liquid bandage in the air for 5 min, forming a robust structure with strong interface bonding between different layers.

Characterizations

The resistance was measured by a DAQ6510 data acquisition/multi-meter system. The tiny voltage variance in **Fig. 3d** was calculated by measuring the voltage of a fixed value resistor which connected in series with the triboelectric nanogenerator (the voltage was measured by PL3516/P Powerlab 16/35, which owns much lower noise signal and higher sampling rate than the DAQ6510 multimeter system).

Mechanical simulation

The finite element analysis commercial software ABAQUS (Analysis User's Manual 2016) was utilized to design the layout of strain sensor and study the corresponding mechanical performance. The objective was to decrease the strain level in Au layer under different typical loads (stretching, bending and twisting). The phantom skin was modeled by hexahedron elements (C3D8R) while the thin Au, Cr, LB and PI layers was modeled by shell elements (S4R). The minimal element size was 1/4th of the width of the Au wires (50 μm), which ensured the convergence of the mesh, and the accuracy of the simulation results. The elastic modulus (E) and Poisson's ratio (ν) used in the analysis were EAu=78 GPa, νAu =0.41; EPI =2.5 GPa, νPI =0.34; Eskin=60 kPa, νskin=0.5; EGr=294 GPa, νGr =0.21 and ELB=85 MPa, νLB=0.42.

DECLARATIONS

Author contributions

Wrote and reviewed the manuscript: Wong T, Yiu C, Zhou J, Song Z, Liu Y, Zhao L, Yao K, Park W, Yoo W, Song E, Xie Z, Yu X

Availability of data and materials

Not applicable.

Financial support and sponsorship

This work was supported by City University of Hong Kong (Grants No. 9610423, 9667199, 9667221, 9680322), Research Grants Council of the Hong Kong Special Administrative Region (Grant No. 21210820, 11213721), Shenzhen Science and Technology Innovation Commission (Grant No. JCYJ20200109110201713). Z.X. acknowledges the support from the National Natural Science Foundation of China (Grant No. 12072057), LiaoNing Revitalization Talents Program (Grant No. XLYC2007196), and Fundamental Research Funds for the Central Universities (Grant No. DUT20RC(3)032). E.S. acknowledged the support from Shanghai Municipal Science and Technology Major Project (No.2018SHZDZX01), ZJ Lab, and Shanghai Center for Brain Science and Brain-Inspired Technology.

Conflicts of interest

All authors declared that there are no conflicts of interest.

Consent for publication

Not applicable.

Ethical approval and consent to participate

Not applicable.

Consent for publication

Not applicable.

Copyright

REFERENCE

1. Yeo, W.H., et al., Multifunctional epidermal electronics printed directly onto the skin. Advanced materials, 2013. 25(20): p. 2773-2778. DOI:10.1002/adma.201204426
2. Jeong, J.W., et al., Materials and optimized designs for human-machine interfaces via epidermal electronics. Advanced Materials, 2013. 25(47): p. 6839-6846. DOI:10.1002/adma.201301921
3. Zhu, Z., R. Li, and T. Pan, Imperceptible epidermal–iontronic interface for wearable sensing. Advanced materials, 2018. 30(6): p. 1705122. DOI:10.1002/adma.201705122
4. Liu, Y., et al., Epidermal mechano-acoustic sensing electronics for cardiovascular diagnostics and human-machine interfaces. Science Advances, 2016. 2(11): p. e1601185. DOI: 10.1126/sciadv.1601185
5. Reeder, J.T., et al., Waterproof, electronics-enabled, epidermal microfluidic devices for sweat collection, biomarker analysis, and thermography in aquatic settings. Science advances, 2019. 5(1): p. eaau6356. DOI: 10.1126/sciadv.aau6356
6. Yu, X., et al., Skin-integrated wireless haptic interfaces for virtual and augmented reality. Nature, 2019. 575(7783): p. 473-479. DOI:10.1038/s41586-019-1687-0
7. Yeo, J.C. and C.T. Lim, Emerging flexible and wearable physical sensing platforms for healthcare and biomedical applications. Microsystems & Nanoengineering, 2016. 2(1): p. 1-19. DOI: 10.1038/micronano.2016.43
8. Liu, Y., et al., Epidermal electronics for respiration monitoring via thermo-sensitive measuring. Materials Today Physics, 2020: p. 100199. DOI: 10.1016/j.mtphys.2020.100199
9. Kim, C.H., et al., Simple and Cost-effective Microfabrication of Flexible and Stretchable Electronics for Wearable Multi-functional Electrophysiological Monitoring. 2021. DOI: 10.21203/rs.3.rs-395029/v1
10. Guo, J., et al., Morphological Hydrogel Microfibers with MXene Encapsulation for Electronic Skin. Research, 2021. 2021. DOI: 10.34133/2021/7065907
11. Liu, Y., et al., Skin-integrated graphene-embedded lead zirconate titanate rubber for energy harvesting and mechanical sensing. Advanced Materials Technologies, 2019. 4(12): p. 1900744. DOI: 10.1002/admt.201900744
12. Tzou, H. and C. Tseng, Distributed piezoelectric sensor/actuator design for dynamic measurement/control of distributed parameter systems: a piezoelectric finite element

386 approach. Journal of sound and vibration, 1990. 138(1): p. 17-34. DOI:
387 10.1016/0022-460X(90)90701-Z
388 13. Ng, T. and W. Liao, Sensitivity analysis and energy harvesting for a self-powered
389 piezoelectric sensor. Journal of Intelligent Material Systems and Structures, 2005.
390 16(10): p. 785-797. DOI: 10.1177/1045389X05053151
391 14. Liu, Y., et al., Electronic Skin from High-Throughput Fabrication of Intrinsically
392 Stretchable Lead Zirconate Titanate Elastomer. Research, 2020. 2020. DOI:
393 10.34133/2020/1085417
394 15. Wang, X., et al., Self-powered high-resolution and pressure-sensitive triboelectric
395 sensor matrix for real-time tactile mapping. Advanced materials, 2016. 28(15): p.
396 2896-2903. DOI: 10.1002/adma.201503407
397 16. An, T., et al., Self-powered gold nanowire tattoo triboelectric sensors for soft
398 wearable human-machine interface. Nano Energy, 2020. 77: p. 105295. DOI:
399 10.1016/j.nanoen.2020.105295
400 17. Wu, M., et al., Thin, soft, skin-integrated foam-based triboelectric nanogenerators for
401 tactile sensing and energy harvesting. Materials Today Energy, 2021. 20: p. 100657.
402 DOI: 10.1016/j.mtener.2021.100657
403 18. Yiu, C., et al., Skin-Like Strain Sensors Enabled by Elastomer Composites for
404 Human–Machine Interfaces. Coatings, 2020. 10(8): p. 711. DOI:
405 10.3390/coatings10080711
406 19. Yan, C., et al., Highly stretchable piezoresistive graphene–nanocellulose nanopaper
407 for strain sensors. Advanced materials, 2014. 26(13): p. 2022-2027. DOI:
408 10.1002/adma.201304742
409 20. Pacelli, M., L. Caldani, and R. Paradiso. Textile piezoresistive sensors for
410 biomechanical variables monitoring. in 2006 International Conference of the IEEE
411 Engineering in Medicine and Biology Society. 2006. IEEE. DOI:
412 10.1109/IEMBS.2006.259287
413 21. Hu, N., et al., Piezoresistive strain sensors made from carbon nanotubes based
414 polymer nanocomposites. Sensors, 2011. 11(11): p. 10691-10723. DOI:
415 10.3390/s111110691
416 22. Zhu et al., Recent progress in flexible tactile sensor systems: from design to
417 application, Soft Sci 2021;1:3. DOI: 10.20517/ss.2021.02
418 23. Liu, Y., et al., Recent progress on flexible nanogenerators toward self-powered
419 systems. InfoMat, 2020. 2(2): p. 318-340. DOI: 10.1002/inf2.12079
420 24. Wang, L., et al., A metal-electrode-free, fully integrated, soft triboelectric sensor
421 array for self-powered tactile sensing. Microsystems & Nanoengineering, 2020. 6(1):
422 p. 1-9. DOI: 10.1038/s41378-020-0154-2

25. Zhou, Y., et al., Highly sensitive, self-powered and wearable electronic skin based on pressure-sensitive nanofiber woven fabric sensor. Scientific reports, 2017. 7(1): p. 1-9. DOI: 10.1038/s41598-017-13281-8
26. Lou, Z., et al., Recent progress of self-powered sensing systems for wearable electronics. Small, 2017. 13(45): p. 1701791. DOI: 10.1002/smll.201701791
27. Wang, Y., Y. Wang, and Y. Yang, Graphene–Polymer Nanocomposite-Based Redox-Induced Electricity for Flexible Self-Powered Strain Sensors. Advanced Energy Materials, 2018. 8(22): p. 1800961. DOI: 10.1002/aenm.201800961
28. Lu, Y., et al., Recent developments in bio-monitoring via advanced polymer nanocomposite-based wearable strain sensors. Biosensors and bioelectronics, 2019. 123: p. 167-177. DOI: 10.1016/j.bios.2018.08.037
29. Wang, X., et al., A highly stretchable transparent self-powered triboelectric tactile sensor with metallized nanofibers for wearable electronics. Advanced Materials, 2018. 30(12): p. 1706738. DOI: 10.1002/adma.201706738
30. Zhao, G., et al., Transparent and stretchable triboelectric nanogenerator for self-powered tactile sensing. Nano Energy, 2019. 59: p. 302-310. DOI: 10.1016/j.nanoen.2019.02.054
31. Yang, M., et al., A Fully Self-Healing Piezoelectric Nanogenerator for Self-Powered Pressure Sensing Electronic Skin. Research, 2021. 2021. DOI: 10.34133/2021/9793458
32. Shu, Y. and I. Lien, Analysis of power output for piezoelectric energy harvesting systems. Smart materials and structures, 2006. 15(6): p. 1499. DOI:10.1088/0964-1726/15/6/001
33. Feng, W., et al., Sensitive electronic-skin strain sensor array based on the patterned two-dimensional α-In2Se3. Chemistry of Materials, 2016. 28(12): p. 4278-4283. DOI: 10.1021/acs.chemmater.6b01073
34. Park, J., et al., Tactile-direction-sensitive and stretchable electronic skins based on human-skin-inspired interlocked microstructures. ACS nano, 2014. 8(12): p. 12020-12029. DOI: 10.1021/nn505953t
35. Lipomi, D.J., et al., Skin-like pressure and strain sensors based on transparent elastic films of carbon nanotubes. Nature nanotechnology, 2011. 6(12): p. 788-792. DOI: 10.1038/nnano.2011.184
36. Cheng, Y., et al., Stretchable electronic skin based on silver nanowire composite fiber electrodes for sensing pressure, proximity, and multidirectional strain. Nanoscale, 2017. 9(11): p. 3834-3842. DOI: 10.1039/C7NR00121E

458 37. Kanao, K., et al., Highly selective flexible tactile strain and temperature sensors
459 against substrate bending for an artificial skin. Rsc Advances, 2015. 5(38): p. 30170-
460 30174. DOI: 10.1039/C5RA03110A
461
462 38. Gong, S., et al., Highly stretchy black gold E-Skin nanopatches as highly sensitive
463 wearable biomedical sensors. Advanced Electronic Materials, 2015. 1(4): p. 1400063.
464 DOI: 10.1002/aelm.201400063
465 39. Luo, N., et al., Hollow-structured graphene–silicone-composite-based piezoresistive
466 sensors: Decoupled property tuning and bending reliability. Advanced materials,
467 2017. 29(40): p. 1702675. DOI: 10.1002/adma.201702675
468 40. Chen, H., et al., Fingertip-inspired electronic skin based on triboelectric sliding
469 sensing and porous piezoresistive pressure detection. Nano Energy, 2017. 40: p. 65-
470 72. DOI: 10.1016/j.nanoen.2017.08.001
471 41. Niu, D., et al., Graphene-elastomer nanocomposites based flexible piezoresistive
472 sensors for strain and pressure detection. Materials Research Bulletin, 2018. 102: p.
473 92-99. DOI: 10.1016/j.materresbull.2018.02.005
474 42. Canavese, G., et al. Comprehensive characterization of large piezoresistive variation
475 of Ni-PDMS composites. in Applied mechanics and materials. 2012. Trans Tech Publ.
476 DOI: 10.4028/www.scientific.net/AMM.110-116.1336
477 43. Cai, G., et al., Extremely stretchable strain sensors based on conductive self-healing
478 dynamic cross-links hydrogels for human-motion detection. Advanced Science, 2017.
479 4(2): p. 1600190. DOI: 10.1002/advs.201600190
480 44. Jing, X., et al., Biocompatible, self-healing, highly stretchable polyacrylic
481 acid/reduced graphene oxide nanocomposite hydrogel sensors via mussel-inspired
482 chemistry. Carbon, 2018. 136: p. 63-72. DOI: 10.1016/j.carbon.2018.04.065
483 45. Liu, S. and L. Li, Ultrastretchable and self-healing double-network hydrogel for 3D
484 printing and strain sensor. ACS Applied Materials & Interfaces, 2017. 9(31): p.
485 26429-26437. DOI: 10.1021/acsami.7b07445
486 46. Yin, F., et al., Flexible and highly sensitive artificial electronic skin based on
487 graphene/polyamide interlocking fabric. Journal of Materials Chemistry C, 2018.
488 6(25): p. 6840-6846. DOI: 10.1039/C8TC00839F
489 47. Zhao, L., et al., Construction of sandwich-like porous structure of graphene-coated
490 foam composites for ultrasensitive and flexible pressure sensors. Nanoscale, 2019.
491 11(21): p. 10229-10238. DOI: 10.1039/C9NR02672J
492 48. Nie, P., et al., High-performance piezoresistive electronic skin with bionic
493 hierarchical microstructure and microcracks. ACS applied materials & interfaces,
494 2017. 9(17): p. 14911-14919. DOI: 10.1021/acsami.7b01979

49. Hsu, M.-S., et al., Gold nanostructures on flexible substrates as electrochemical dopamine sensors. ACS applied materials & interfaces, 2012. 4(10): p. 5570-5575. DOI: 10.1021/am301452b
50. Zhu, Y. and J. Moran-Mirabal, Highly bendable and stretchable electrodes based on micro/nanostructured gold films for flexible sensors and electronics. Advanced Electronic Materials, 2016. 2(3): p. 1500345. DOI: 10.1002/aelm.201500345
51. Li, Y.-Q., et al., Flexible wire-shaped strain sensor from cotton thread for human health and motion detection. Scientific reports, 2017. 7(1): p. 1-7. DOI: 10.1038/srep45013 (2017)
52. Sankar, V., et al., Waterproof flexible polymer-functionalized graphene-based piezoresistive strain sensor for structural health monitoring and wearable devices. ACS omega, 2020. 5(22): p. 12682-12691. DOI: 10.1021/acsomega.9b04205
53. Wang, X., et al., Highly stretchable and wearable strain sensor based on printable carbon nanotube layers/polydimethylsiloxane composites with adjustable sensitivity. ACS applied materials & interfaces, 2018. 10(8): p. 7371-7380. DOI:10.1021/acsami.7b17766
54. Zheng, Y., et al., High-performance wearable strain sensor based on graphene/cotton fabric with high durability and low detection limit. ACS applied materials & interfaces, 2019. 12(1): p. 1474-1485. DOI: 10.1021/acsami.9b17173
55. Zheng, S., et al., Highly sensitive and multifunctional piezoresistive sensor based on polyaniline foam for wearable Human-Activity monitoring. Composites Part A: Applied Science and Manufacturing, 2019. 121: p. 510-516. DOI: 10.1016/j.compositesa.2019.04.014
56. Zhang, C., et al., A simple method of fabricating nickel-coated cotton fabrics for wearable strain sensor. Cellulose, 2018. 25(8): p. 4859-4870. DOI: 10.1007/s10570-018-1893-1